Comparisons of Surface Meteorology and Turbulent Heat Fluxes over the Atlantic: NWP Model Analyses versus Moored Buoy Observations*

BOMIN SUN,+ LISAN YU, AND ROBERT A. WELLER

Department of Physical Oceanography, Woods Hole Oceanographic Institution, Woods Hole, Massachusetts

(Manuscript received 12 October 2001, in final form 28 May 2002)

ABSTRACT

Surface meteorological variables and turbulent heat fluxes in the National Centers for Environmental Prediction–National Center for Atmospheric Research reanalyses 1 and 2 (NCEP1 and NCEP2) and the analysis from the operational system of the European Centre for Medium-Range Weather Forecasts (ECMWF) are compared with high-quality moored buoy observations in regions of the Atlantic including the eastern North Atlantic, the coastal regions of the western North Atlantic, and the Tropics. The buoy latent and sensible heat fluxes are determined from buoy measurements using the recently improved Tropical Ocean Global Atmosphere Coupled Ocean–Atmosphere Response Experiment (TOGA COARE) flux algorithm.

The time mean oceanic heat loss from the model analyses is systematically overestimated in all the regions. The overestimation in latent heat loss ranges from about 14 W m^{-2} (13%) in the eastern subtropical North Atlantic to about 29 W m^{-2} (30%) in the Tropics to about 30 W m^{-2} (49%) in the midlatitude coastal areas, where the overestimation in sensible heat flux reaches about 20 W m^{-2} (60%). Depending upon the region and the NWP model, these systematic overestimations are either reduced, or change to underestimations, or remain unchanged when the TOGA COARE flux algorithm is used to recalculate the fluxes. The bias in surface meteorological variables, one of the major factors related to the biases in the revised NWP heat fluxes, varies with region and NWP analysis. Generally the temperature and humidity biases in the coastal regions are much larger than other regions. In the extratropical regions, NCEP1 and NCEP2 generally show a wet bias, which is mainly responsible for the underestimation in the revised NWP latent heat loss. In the Tropics a dry bias is found in the NWP analyses, particularly in ECMWF and NCEP2, which contributes to the overestimation in the revised NWP latent heat loss. Compared to NCEP1, NCEP2 shows less cold bias in 2-m air temperature and thus less biased sensible heat flux; NCEP2 also shows less humid bias in 2-m humidity in the extratropical regions but more dry bias in 2-m humidity in the Tropics, either of which leads to a more biased latent heat flux in NCEP2.

Despite the significant biases in the NWP surface fields and the poor representation of short-time sea surface temperature variability, the NWP models are able to represent the dominant short-time variability in other basic variables and thus the variability in heat fluxes in the wintertime coastal regions of the western North Atlantic (on timescales of 3–4 days and 1 week) and the northern and southern subtropical regions (on a timescale of about 2 weeks), but ECMWF and particularly the NCEP analyses do not represent well the 2–3-week variability in the tropical Atlantic.

1. Introduction

Accurate basin-scale air–sea heat fluxes are needed to better understand and predict climate change. Numerical weather prediction (NWP) analysis-forecast systems provide 6-hourly fluxes with global coverage. However, uncertainties in model physical parameterizations can lead to uncertainties in surface fluxes from the global NWP analysis-forecast systems. Differences in model and data assimilation configurations also lead to discrepancies in surface fluxes between different analysis products. Evaluation of the representativeness of analysis fluxes is therefore necessary. In spite of the limitation in time and space, high-quality in situ data from surface moorings, ships, and other platforms are able to serve as ''ground truth'' reference data to quantify locally or regionally the uncertainties in model flux products.

Recent data–model analysis comparative studies have been carried out in regions of the World Ocean, including the Arabian Sea (Weller et al. 1998), the tropical Pacific (Weller and Anderson 1996; Smull and McPhaden 1998; Zeng et al. 1998; Wang and McPhaden 2001), the eastern North Atlantic (Moyer and Weller 1997; Josey 2001), the Labrador Sea (Renfrew et al.

* Woods Hole Oceanographic Institution Contribution Number 10596.

+ Current affiliation: National Climatic Data Center, Asheville, North Carolina.

Corresponding author address: Dr. Bomin Sun, National Climatic Data Center, 151 Patton Ave., Asheville, NC 28801.
E-mail: Bomin.Sun@noaa.gov

2002), and others. A global comparative study has also been conducted by Smith et al. (2001) using the high-quality research vessel data during the World Ocean Circulation Experiment (WOCE). These studies found that the ocean turbulent heat losses in model analyses are seriously in error, and these errors are due both to flux algorithms and to bulk variables. Biases in the NWP variables and fluxes are also shown in the comparison using satellite measurements (Curry et al. 1999; Halpern et al. 1999; Chelton 2001). The previous comparison studies also indicate that the factors related to the data–analysis discrepancies can be different at different regions. For example, Wang and McPhaden (2001) indicated that the major contribution to the difference between NWP fluxes and fluxes estimated from the Tropical Atmosphere Ocean (TAO) buoy data in the tropical Pacific stems from the biases in the model meteorological variables, while Renfrew et al. (2002) found that in the Labrador Sea the heat flux algorithms employed in the models are the major source of the data–model analysis disagreement. Careful evaluation is therefore needed to quantify NWP uncertainty at a ''new'' location/region of interest. Furthermore, due to limitations in the duration of high-quality in situ data, little is known about the ability of model analyses to replicate the temporal variability in surface fields.

In this work, surface meteorology and turbulent heat fluxes from the National Centers for Environmental Prediction–National Center for Atmospheric Research (NCEP–NCAR) reanalyses 1 and 2 (NCEP1 and NCEP2; Kalnay et al. 1996; Kanamitsu et al. 2000), and the analysis from the operational system of the European Centre for Medium-Range Weather Forecasts (ECMWF 1994) will be compared to high-quality moored buoy measurements collected from research experiments conducted in regions of the Atlantic Ocean, including the eastern subtropical North Atlantic, the coastal regions of the western North Atlantic, and the low-latitude Atlantic (Fig. 1). NCEP1 and ECMWF products have been widely used in scientific research and cited in various literatures while NCEP2 reanalysis is relatively new. The reanalysis-forecast system in NCEP2 has the same resolution and raw observation data as in NCEP1. The turbulent heat flux algorithm used in NCEP2 is also the same as in NCEP1. However, NCEP2 differs from NCEP1 in the shortwave radiation and cloud parameterizations, and some other parameters prescribed in the atmospheric model. The buoy data are not used in preparing the NWP analyses, except in the case of the Pilot Research Moored Array in the Tropical Atlantic (PIRATA; Servain et al. 1998). The climate regime and ocean state differ from one extratropical site to another, and even in the tropical Atlantic the prevailing climate system differs considerably across the PIRATA array. We have brought together these data in this article, hoping to understand more comprehensively the performance of these NWP analysis-forecast systems to replicate the time mean and temporal variability of surface fields in the Atlantic. The surface fields include latent and sensible heat fluxes and sea surface temperature (SST), air temperature, air humidity, and wind speed. This comparative study is part of our effort to construct a high-quality heat flux product in the Atlantic basin by synthesizing data from model analyses, satellite measurements, and in situ observations using the variational analysis method (Legler et al. 1989; Jones et al. 1995; Yu et al. 2001). Information on uncertainties in model fluxes as well as bulk variables identified by this comparison is needed for this kind of data synthesis.

Section 2 provides an overview of the buoy experiments and data processing along with the Tropical Ocean Global Atmosphere Coupled Ocean–Atmosphere Response Experiment (TOGA COARE) flux algorithm, which is used to calculate buoy latent and sensible heat fluxes. We realize that the parameterized near-surface energy exchange (as well as other physical processes) in the NWP models can strongly impact model bulk variables, and any bias in NWP bulk variables is therefore inseparable from inappropriate air–sea flux parameterizations. However, in order to estimate the relative contributions of biases in bulk variables and in flux algorithms to NWP heat fluxes, we recalculate NWP model fluxes by applying the TOGA COARE algorithm to model bulk variables. In section 3, we first present the time mean heat flux comparison for all the experiments, and then, we analyze, experiment by experiment, the possible factors (e.g., biases in bulk variables and in flux algorithms) related to the time mean heat flux biases. The temporal variability comparison is provided in section 4. We compare NWP model analyses with buoy data on the timescales dominant in the deployment of the experiments we analyze. Conclusions and discussions of the data–model analysis differences are offered in section 5.

2. Buoy datasets and their processing

a. Overview of buoy experiments

The buoy data were collected from the following research experiments (Fig. 1): the Subduction Experiment in the eastern subtropical North Atlantic (Moyer and Weller 1997), the west North Atlantic coastal region experiments including the Severe Environment Surface Mooring (SESMOOR; Crescenti et al. 1991) for the Experiment on Rapidly Intensifying Cyclones over the Atlantic (ERICA), the Coastal Mixing and Optics Experiment (CMO; Galbraith et al. 1999), the 1993 Acoustic Surface Reverberation Experiment (ASREX93; Galbraith et al. 1996), and PIRATA in the low-latitude Atlantic. The Subduction Experiment and the three coastal region experiments were carried out by the Upper Ocean Processes Group of the Woods Hole Oceanographic Institution (WHOI). PIRATA is a multinational program and is designed to better understand ocean–atmosphere interactions in the tropical Atlantic that are relevant to

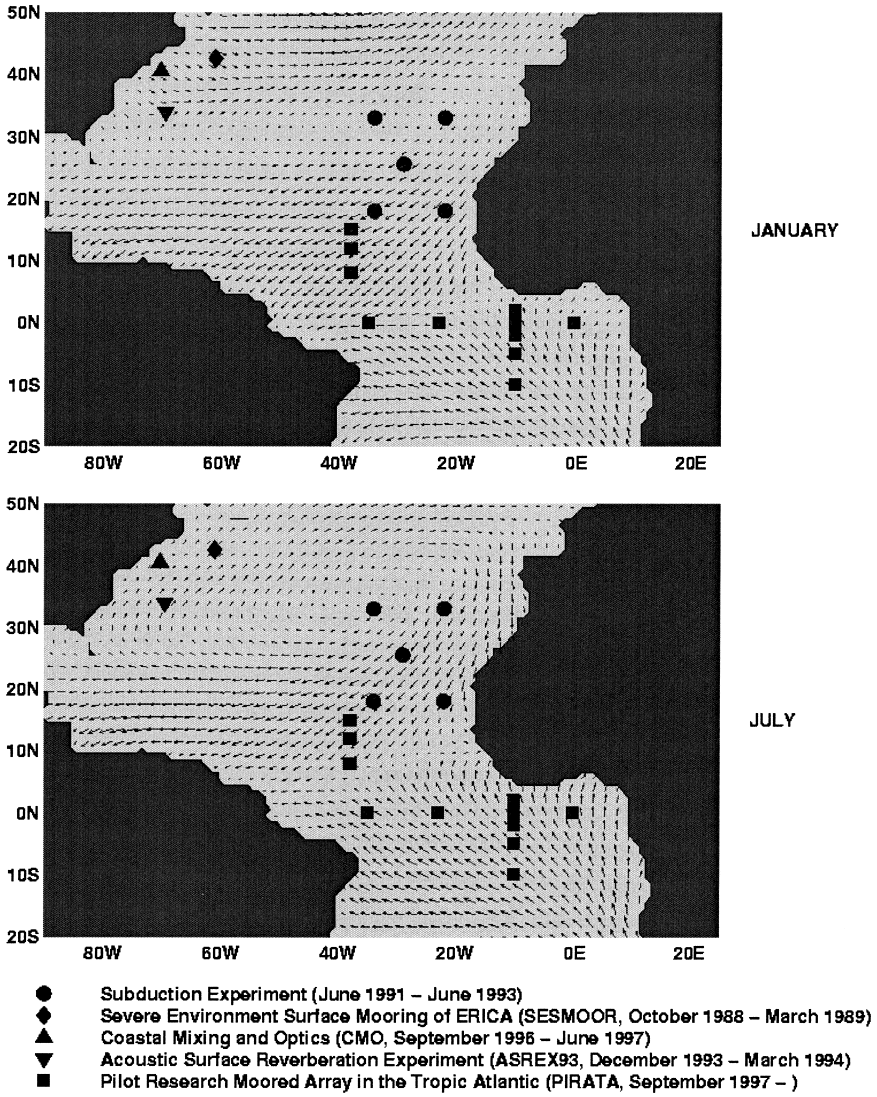

FIG. 1. Locations of moored buoys in the Atlantic used for comparison. The 10-m wind climatology (1988–97) for Jan and Jul from NCEP2 reanalysis is depicted.

regional climate variability on seasonal, interannual, and longer timescales. The buoy (or array) location and the deployment period along with the basic meteorological and oceanic states for each experiment are briefly described below.

1) SUBDUCTION EXPERIMENT

The Subduction Experiment with an array of five buoys was operated between June 1991 and June 1993 in the eastern North Atlantic (18°–33°N, 22°–34°W; Moyer and Weller 1997). The five buoys were located at (33°N, 34°W), (33°N, 22°W), (25.5°N, 29°W), (18°N, 34°W), and (18°N, 22°W) and referred to by their relative directional positions (NW, NE, C, SW, and SE). The buoy array was mainly under the influence of the Azores high pressure system with northeast trades prevailing the entire year. The times when the buoys were on station vary from buoy to buoy. There are a total of 84 months (2640 days) with valid buoy observations from the 2-yr array deployment.

2) COASTAL REGION EXPERIMENTS

SESMOOR was deployed at a position about 300 km southeast of Halifax, Nova Scotia, in 2984 m of water. The buoy location (42.6°N, 61.2°W) was bounded to the south by the Gulf Stream. The mean SST during the deployment period of the 1988–89 winter is about 6.5°C with a strong meridional gradient (approximately 2.5°–3°C for 1° of latitude) occurring around the buoy. In the midlatitude coastal region of the western North Atlantic during wintertime, high-frequency synoptic weather systems move from the cold landmass to the

relatively warm water, resulting in extremely high variability of heat fluxes.

The CMO buoy (40.5°N, 60.3°W) was located over the New England continental shelf about 100 km south of Cape Cod, Massachusetts, in 70 m of water. The deployment period, August 1996–June 1997, was intended to capture the breakdown of oceanic stratification in autumn and its redevelopment in spring. The meteorological condition in wintertime is similar to that in SESMOOR. The mean SST at the buoy location for the record period of 1 October 1996–12 June 1997 was 8°C.

ASREX93 took place in the winter of 1993–94 in the western North Atlantic, roughly halfway between Bermuda and Cape Hatteras, North Carolina. The normal water depth is 5370 m. ASREX93 was intended to improve understanding of near-surface acoustic reverberation in high sea states. The climate and ocean states in ASREX differed from those in SESMOOR and in CMO. The buoy (33.9°N, 69.8°W) was located south of the Gulf Stream and at the western edge of the North Atlantic subtropical high. The time mean SST during the deployment period was 18.9°C. The SST near the buoy site was spatially homogeneous. There were cold weather systems moving from the northwest through the site but not so frequently as in SESMOOR. The atmospheric variability in ASREX93 was also influenced by the southerly flow associated with the North Atlantic subtropical high (Fig. 1). The measurements from January 1994 to March 1994, a total of 82 days, are used in this comparison.

3) PIRATA

The data from the PIRATA array come from 12 moored buoys deployed during the years 1997–2000. The northern buoys are close to the Subduction Experiment buoys, thus extending our study region from the northern to the southern subtropical Atlantic. Across the PIRATA array, the length of data available varies from 30 months to 2–3 months or less. Only a few days of data are available from the buoy at (4°N, 38°W) and thus are not used in this study. The PIRATA array cuts through a wide range of climate regimes and ocean states (Fig. 1). From north to south, the array passes through the northeast trades with low SSTs and frequently clear skies, to the intertropical convergence zone (ITCZ), a region of weak winds, high SSTs, and strong convection, and then into the region of the southeast trades along 10°W. Along the equator, the array extends from the warm pool with high SSTs in the west to the cold tongue in the east with strong equatorial upwelling.

b. Buoy data processing

The basic meteorological variables measured by the meteorological instrumentation on the WHOI buoys include surface pressure, ocean temperature at the depth of 1 m, relative humidity and air temperature at the height of 2.7 m, and wind speed and direction at 3.4 m. The PIRATA array uses the Autonomous Temperature Line Acquisition System (ATLAS) to measure relative humidity and air temperature at 3 m and wind speed and direction at 4 m. (The ATLAS is also used in the TAO array.) The accuracy of buoy measurements has been checked through pre- and postdeployment instrument calibrations. The uncertainties in the surface meteorological variables and in the derived heat fluxes caused by the instrumental biases for the WHOI buoys and PIRATA are described, respectively, in Moyer and Weller (1997) and Wang and McPhaden (2001). In this study, we derive air specific humidity from the relative humidity and air temperature using TeTen's formula (Bolton 1980). The heights of air temperature (humidity) and wind speed from NCEP1 and NCEP2 reanalyses and operational ECMWF analysis are 2 and 10 m, respectively. For purposes of comparison we adjust the buoy wind speed at 3.4 or 4 m to the 10-m height of the NWP winds using the COARE2.6a algorithm (Bradley et al. 2000). The 2-m height-adjusted buoy air temperature and humidity are very close in value to the unadjusted ones, and therefore the measurement air temperature and humidity at 2.7 or 3 m are directly used in this comparison.

The buoy meteorological data in use are 15-min-averaged measurements from the WHOI buoys and 10-min averages from PIRATA. In the NWP analyses, the meteorological variables are daily averages of four measurements (0000, 0600, 1200, and 1800 UTC) and the heat fluxes are daily averages of four 6-h accumulations. In an effort to evaluate the performance of the assimilation products to replicate the surface fields from the buoys on timescales as short as daily, daily values of buoy bulk variables are calculated by averaging those four 15-min (10 min) block data coincident with the model analyses times, and the daily buoy fluxes are obtained by averaging all the 15-min (10 min) block flux values within a day. The monthly values are calculated from these daily data for both buoy measurements and model analyses.

In general, the data from the model analyses at the nearest grid point to the buoy measurement location are used for comparison if that grid point is within 75 km of the research buoy. Otherwise, the model value is bilinearly interpolated (inversely weighted by distance) from values of the surrounding four grid points. Special attention is paid to the buoys in the midlatitude coastal regions of the western North Atlantic, where surface fields change strongly and inhomogeneously in space. In those cases, we carefully examine the model and buoy data and use (or put more weight on) the value from the grid point that most closely replicates the buoy observations, to obtain the representative model value. For example, the CMO buoy was located over the continental shelf and was about 100 km away from the northern boundary of the Gulf Stream. The shelf SST was

relatively spatially homogeneous. We therefore use only the values of the model grid points also located in the shelf to get the NWP analysis values at the buoy location.

c. COARE2.6a flux algorithm

The buoy turbulent heat fluxes are estimated using the buoy bulk variables and the COARE algorithm, COARE2.6a (Bradley et al. 2000), an improved version of COARE2.5b (Fairall et al. 1996). Compared to COARE2.5b, the COARE2.6a algorithm is expected to increase turbulent heat fluxes under strong and weak winds. The COARE algorithm incorporates the cool skin and warm layer correction models, which allow us to derive skin temperature from buoy-measured 1-m bulk temperature with the input of solar and infrared radiative fluxes in addition to other basic meteorological variables. Sea surface skin temperatures at the WHOI buoys are thus calculated from the COARE2.6a algorithm. Throughout this paper, SSTs from the WHOI buoys are represented by the estimated skin temperatures. Due to the lack of downward longwave flux measurements in PIRATA, the skin temperature cannot be directly derived from the COARE algorithm, and the buoy-measured 1-m bulk temperature is used in the flux calculation instead. Across the PIRATA array, the time mean wind speeds are generally above 6 m s^{-1} and the cool skin effect is expected to be about 0.17°C (Donlon et al. 1999). As a result, the use of bulk surface temperature instead of skin surface temperature may increase PIRATA buoy latent heat flux loss by about 5 W m^{-2}. And, due to the small magnitude of the air–sea temperature gradient and thus of sensible heat flux in the Tropics, the effect of using the bulk surface temperature on PIRATA buoy sensible heat flux can be significant. The PIRATA heat flux comparison therefore must be conducted with caution. In this article, a negative value of flux represents the loss of ocean heat to the atmosphere, and a positive value represents the ocean heat gain.

3. Time mean comparison

a. Comparison of turbulent heat fluxes

Figure 2 shows the time mean latent and sensible heat fluxes for the five experiments considered. In each panel of Fig. 2, the black bars represent buoy fluxes and NWP fluxes including NCEP1, NCEP2, and ECMWF fluxes, and the gray ones denote the revised NWP fluxes by applying the COARE2.6a algorithm to the NWP bulk variables. The time mean difference and plus and minus one standard deviation of daily difference between the NWP analyses and buoy surface fields for each experiment are listed in Table 1. The numbers shown in Fig. 2 and listed in Table 1 for the Subduction Experiment and PIRATA are array-averaged values. As demonstrated in Fig. 2, relative to buoy values the time mean ocean heat losses from the three model analyses are unanimously overestimated in all the experiments in spite of their differences in geographic location and prevailing meteorological and oceanic conditions. For latent heat flux, the amounts of overestimation in the NWP analyses are generally less than 20% in the Subduction Experiment and ASREX93 while larger biases are shown in CMO, SESMOOR, and PIRATA. For example, the amounts of overestimation for NCEP1, NCEP2, and ECMWF in PIRATA are 23 (25%), 31 (33%), and 32 W m^{-2} (34%). For sensible heat flux, the NWP analyses generally show an overestimation of less than 5 W m^{-2} in the Subduction Experiment and PIRATA while significant biases are noticed in the coastal region experiments. For example, NCEP1, NCEP2, and ECMWF overestimate sensible heat loss by 26 (51%), 19 (37%), and 36 W m^{-2} (68%), respectively, in SESMOOR. Figure 3 also indicates that among the three NWP model analyses, ECMWF exhibits the largest bias in latent heat loss and NCEP2 shows improvement over NCEP1 in sensible heat flux but not in latent heat flux, which will be explained in the next section.

Similar analyses are conducted for all the buoys in the Subduction Experiment array and the PIRATA array. In the Subduction Experiment the overestimated latent heat loss in each of the three model analyses is persistent across the array with a larger bias in the southern buoys. The time mean comparison across the PIRATA array is shown in Fig. 3. Despite the different climate regimes in which the PIRATA buoys are located and the different durations of the sample data, the time mean turbulent heat losses in NCEP1, NCEP2, and ECMWF are overestimated across virtually the entire array, except at (2°N, 10°W) where the three model analyses slightly underestimate the sensible heat loss. As mentioned in section 2, the use of bulk surface temperature instead of skin temperature in PIRATA buoy flux calculation can overestimate buoy latent heat loss by about 5 W m^{-2} and sensible heat loss by 2 W m^{-2}. Hence, the amounts of overestimation in NWP fluxes across the PIRATA array shown in Figs. 1 and 2 are a little conservative.

b. Comparison of basic meteorological variables and flux algorithms

The standard deviations of the daily difference in heat fluxes as well as in bulk variables for WHOI and PIRATA buoys (Table 1) are all beyond their instrumental uncertainties (Moyer and Weller 1997; Wang and McPhaden 2001). The errors in the NWP model surface heat fluxes are thus directly related to the biases in bulk variables and/or to the uncertainties in the bulk aerodynamic formulas used to compute the fluxes although the mechanism responsible for the biases in NWP bulk variables is complicated. In order to assess the relative contribution of biases in bulk variables to model turbulent heat fluxes, we recalculate (and thus revise) NWP

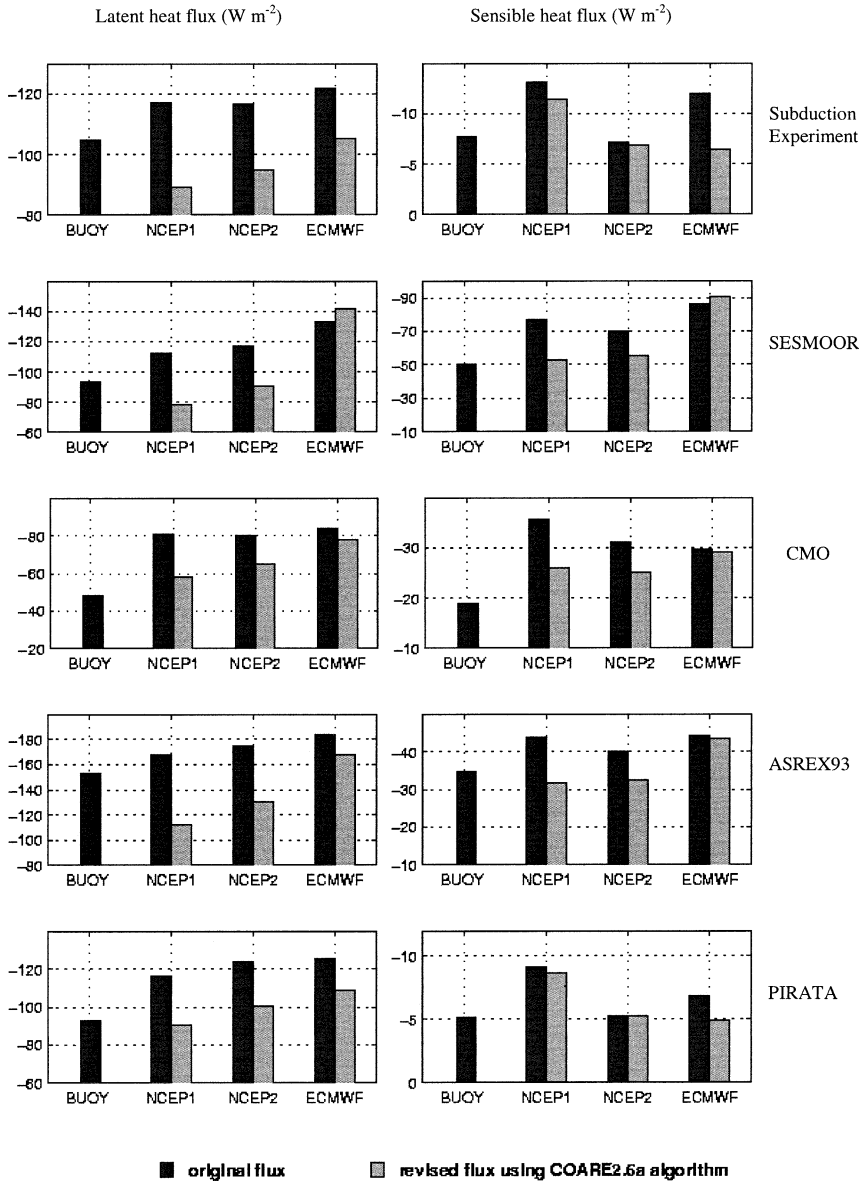

FIG. 2. Time mean surface heat fluxes for buoy data, NCEP1, NCEP2, and ECMWF in the Subduction Experiment, SESMOOR, CMO, ASREX93, and PIRATA. The black bars represent the original heat fluxes while the gray bars denote the revised analyses heat fluxes by applying the COARE2.6a bulk algorithm to the analyses bulk variables. The left column is for latent heat flux and the right column for sensible heat flux.

fluxes by applying the COARE2.6a algorithm to their bulk variables. Next we analyze, experiment by experiment, the contributions of biases in NWP model flux algorithms and in bulk variables to the biases in NWP heat fluxes.

1) SUBDUCTION EXPERIMENT

The revised NCEP1, NCEP2, and ECMWF latent heat fluxes calculated using the COARE2.6a algorithm are smaller in magnitude than their original ones by 28, 21, and 17 W m^{-2}, respectively. As a result, as shown in Fig. 2 the revised ECMWF heat fluxes show close agreement with buoy values while the revised latent heat losses in NCEP1 and NCEP2 become underestimated by 16 and 10 W m^{-2}, respectively. These underestimations are caused primarily by the low bias in air–sea humidity difference due to the wet bias in air humidity, combined with the low bias in wind speed (Table 1). The larger bias in the revised NCEP1 latent (sensible) heat flux relative to NCEP2 is due to the larger bias in air humidity (air temperature) in NCEP1.

TABLE 1. Time means of latent and sensible heat fluxes, SST (T_{sea}), air temperature (T_{air}), air humidity (Q_{air}), air–sea temperature difference $T_{sea} - T_{air}$), air–sea humidity difference ($Q_{sea} - Q_{air}$), and 10-m wind speed for buoy data. Values are also listed as time mean difference and ±1 std dev of daily difference between the NWP analyses and buoy values. Array-averaged values are shown for the Subduction Experiment and PIRATA. The numbers of days with buoy data available are 2640, 139, 226, 82, and 2585 in the Subduction Experiment, SESMOOR, CMO, ASREX93, and PIRATA, respectively.

Source	Latent heat flux (W m^{-2})	Sensible heat flux (W m^{-2})	T_{sea} (°C)	T_{air} (°C)	Q_{air} (g kg^{-1})	$T_{sea} - T_{air}$ (°C)	$Q_{sea} - Q_{air}$ (g kg^{-1})	Wind speed (m s^{-1})
Subduction buoy	−105	−8	22.1	21.4	12.3	0.7	4.0	6.9
NCEP1—buoy	−12 ± 29	−5 ± 10	0.0 ± 0.4	−0.3 ± 0.5	0.6 ± 0.8	0.3 ± 0.6	−0.5 ± 0.8	−0.4 ± 1.1
NCEP2—buoy	−12 ± 30	1 ± 8	0.0 ± 0.4	0.1 ± 0.5	0.3 ± 0.7	−0.1 ± 0.5	−0.3 ± 0.7	−0.4 ± 1.2
ECMWF—buoy	−17 ± 36	−4 ± 7	0.1 ± 0.5	0.1 ± 0.7	−0.1 ± 0.9	−0.1 ± 0.5	0.1 ± 1.0	−0.4 ± 1.1
SESMOOR buoy	−93	−51	6.5	4.0	4.3	2.5	2.0	9.6
NCEP1—buoy	−20 ± 59	−26 ± 54	1.6 ± 2.0	1.3 ± 1.1	0.8 ± 0.6	0.3 ± 1.7	−0.3 ± 1.1	0.2 ± 1.8
NCEP2—buoy	−24 ± 66	−19 ± 58	1.5 ± 2.0	1.2 ± 1.3	0.6 ± 0.7	0.3 ± 1.9	−0.1 ± 1.2	0.8 ± 2.1
ECMWF—buoy	−40 ± 59	−36 ± 46	3.3 ± 2.3	0.8 ± 1.8	0.1 ± 0.7	2.5 ± 2.5	1.2 ± 1.2	0.4 ± 2.0
CMO buoy	−49	−19	8.0	7.0	5.4	1.0	1.4	8.3
NCEP1—buoy	−33 ± 41	−17 ± 37	0.2 ± 1.1	−0.0 ± 1.2	0.1 ± 0.6	0.3 ± 1.2	0.1 ± 0.7	0.4 ± 1.7
NCEP2—buoy	−31 ± 31	−12 ± 25	−0.1 ± 0.9	−0.3 ± 0.7	−0.3 ± 0.4	0.3 ± 0.8	0.3 ± 0.5	0.1 ± 1.2
ECMWF—buoy	−35 ± 31	−11 ± 21	0.7 ± 1.2	0.1 ± 0.9	−0.3 ± 0.4	0.6 ± 1.1	0.7 ± 0.7	−0.3 ± 1.2
ASREX93 buoy	−153	−35	18.9	16.4	8.8	2.5	4.5	8.8
NCEP1—buoy	−14 ± 32	−9 ± 24	−0.7 ± 0.5	−0.4 ± 0.8	0.7 ± 0.9	−0.3 ± 0.7	−1.3 ± 0.8	0.1 ± 1.5
NCEP2—buoy	−22 ± 38	−5 ± 23	−0.7 ± 0.5	−0.2 ± 0.6	0.6 ± 0.7	−0.5 ± 0.6	−1.2 ± 0.7	1.2 ± 1.4
ECMWF—buoy	−30 ± 33	−9 ± 17	−0.2 ± 0.6	−0.5 ± 0.8	−0.1 ± 0.5	0.4 ± 1.0	−0.0 ± 0.6	0.6 ± 1.2
PIRATA buoy	−93	−5	26.4	26.1	17.4	0.5	3.7	6.7
NCEP1—buoy	−24 ± 28	−4 ± 6	0.0 ± 0.3	−0.2 ± 0.5	−0.1 ± 0.7	0.3 ± 0.4	0.2 ± 0.8	−0.6 ± 1.1
NCEP2—buoy	−31 ± 33	−0 ± 5	0.0 ± 0.3	0.0 ± 0.5	−0.3 ± 0.7	0.0 ± 0.5	0.4 ± 0.8	−0.4 ± 1.2
ECMWF—buoy	−32 ± 23	−2 ± 5	0.0 ± 0.4	0.0 ± 0.5	−1.0 ± 0.6	0.0 ± 0.5	1.0 ± 0.7	−0.7 ± 0.8

2) COASTAL REGION EXPERIMENTS

SESMOOR. The overestimated heat losses in NCEP1 and NCEP2 are drastically reduced when the COARE2.6a algorithm is applied to their bulk variables: the latent and sensible heat losses are reduced by 35 and 24 W m^{-2} for NCEP1, and 27 and 14 W m^{-2} for NCEP2. Relative to buoy values, the revised latent heat loss in NCEP1 thus becomes underestimated (by 15 W m^{-2}) and the revised sensible heat losses in NCEP1 and NCEP2 and the revised NCEP2 latent heat loss tend to be close to buoy values. It is noteworthy that the revised ECMWF fluxes, instead of being largely reduced as in the Subduction Experiment or in the NCEP model analyses, become larger only by 8% in magnitude relative to their original ones.

The overestimated heat losses in ECMWF are caused mainly by the extremely warm bias of 3.3°C in SST, which leads to a bias of 1.2 g kg^{-1} in air–sea humidity difference and a bias of 2.5°C in air–sea temperature difference despite the positive biases in air temperature and humidity (Table 1). NCEP2 also shows warm biases in SST and air temperature and a wet bias in air humidity. However, in contrast to the biases in ECMWF, the SST bias in NCEP2 is much smaller while the biases in air temperature and humidity in NCEP2 are larger. Thus, the errors in NCEP2 air–sea humidity and temperature differences largely offset each other, leading to small biases in the revised NCEP2 fluxes. The errors in temperature, humidity, and wind speed in NCEP1 are similar to those in NCEP2 except for a more humid bias in NCEP1, causing a relatively large underestimation in the revised NCEP1 latent heat loss.

The bias in the NWP SSTs in SESMOOR is remarkable and needs additional discussion. We compared the SSTs from the three model analyses and the buoy with collocated SSTs from measurements of the Advanced Very High Resolution Radiometer (AVHRR) on the days with data available during the SESMOOR deployment. Due to frequently cloudy skies, there were only 20 days with AVHRR data available during the 139-day buoy deployment. It is found that, after taking into account the cool skin effect, the 20-day-averaged AVHRR SST is only slightly higher (by 0.3°C) than the buoy value while it is lower than the NCEP1, NCEP2, and ECMWF by 0.8°, 0.9°, and 2.8°C, respectively. This independent validation confirms the large warm biases in the NWP SSTs, particularly in the ECMWF analysis. Also, the big biases in the SST analyses may be partly contributed by the inability of the models' coarse resolution to properly resolve the strong surface temperature gradients along the wintertime coastal region.

CMO. As in SESMOOR, the revised ECMWF heat fluxes using the COARE2.6a algorithm remain practically unchanged while the revised heat fluxes in NCEP1 and NCEP2 are much smaller in magnitude than originally but still show overestimations of 9 and 16 W m^{-2} for latent heat and 7 and 6 W m^{-2} for sensible heat. Generally, the biases in NWP meteorological variables in CMO are smaller than the corresponding ones in SESMOOR. ECMWF shows a low wind bias of 0.3 m s^{-1} and a warm bias of 0.7°C in SST, which should be

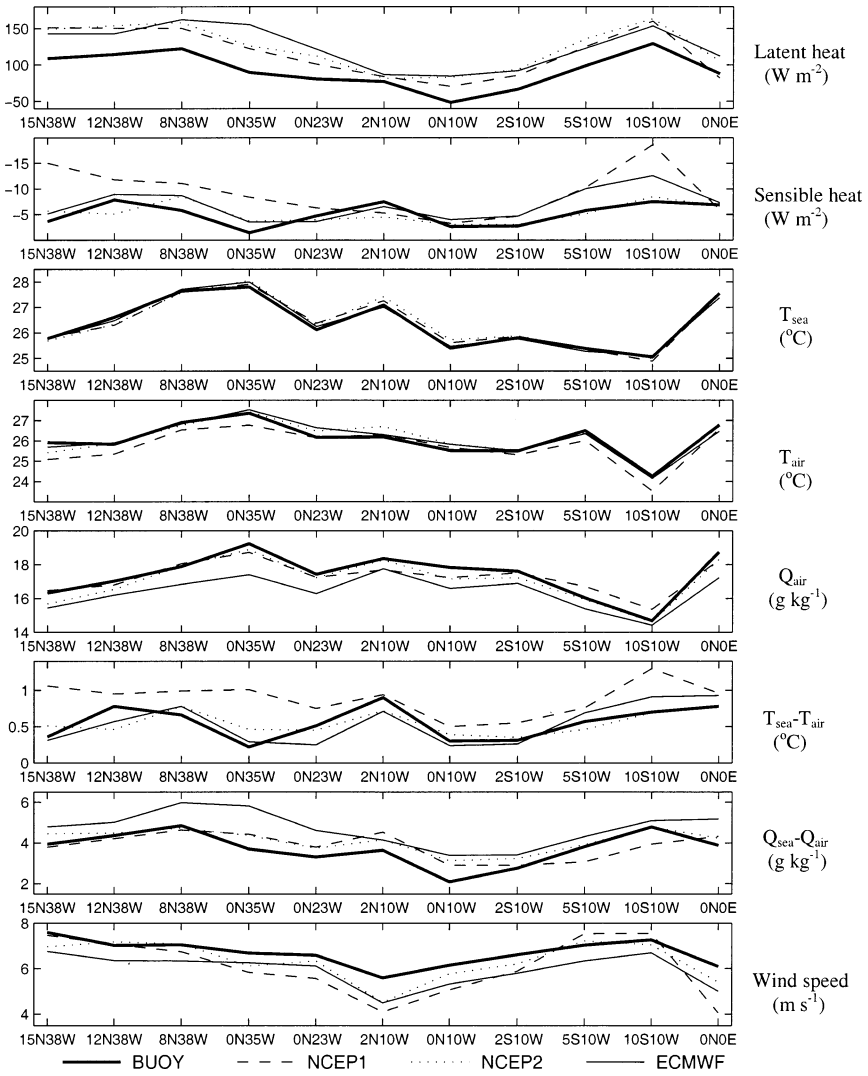

FIG. 3. Time means of latent heat flux, sensible heat flux, SST (T_{sea}), air temperature (T_{air}), air humidity (Q_{air}), air–sea temperature difference ($T_{sea} - T_{air}$), air–sea humidity difference ($Q_{sea} - Q_{air}$), and 10-m wind speed for buoy data, NCEP1, NCEP2, and ECMWF across the PIRATA array.

primarily responsible for the excessive heat losses. The overestimated heat losses in the revised NCEP1 and NCEP2 flux calculations are caused, as shown in Table 1, by the positive biases in air–sea humidity and temperature differences along with the high wind speed bias. However, the biases in NCEP2 differ somehow from those in NCEP1. In NCEP2, the atmosphere is biased slightly cold and dry while NCEP1 shows a warm bias of 0.2°C in SST and a slightly wet bias in air humidity.

ASREX93. The situation in ASREX93 is similar to SESMOOR. The latent heat losses in NCEP1 and NCEP2 are reduced by using the COARE2.6a algorithm by 45 and 56 W m^{-2}, respectively, and thus become underestimated (by 45 and 24 W m^{-2}) relative to the buoy value. The COARE2.6a algorithm reduces the NCEP1 and NCEP2 sensible heat losses by 8 and 12 W m^{-2}, thus bringing the revised sensible heat fluxes closer to buoy flux. For ECMWF, similar to what we found in SESMOOR and CMO, the COARE2.6a algorithm does not significantly change the heat losses. This suggests that the ECMWF flux algorithm behaves similar to the COARE2.6a algorithm under the conditions of strong air–sea temperature gradients and strong winds such as in the wintertime coastal regions.

As shown in Table 1, the ASREX93 SSTs and air temperatures in the three NWP analyses are biased cold with a larger SST bias of 0.7°C in NCEP1 and NCEP2 and a larger air temperature bias of 0.5°C in ECMWF. NCEP1 and NCEP2 show a wet bias of 0.6–0.7 g kg^{-1} in air humidity while the air humidity from ECMWF is close to the buoy value. The 10-m wind speeds in the

three analyses are all biased strong, with the largest bias of 1.2 m s^{-1} in NCEP2. The larger underestimations in the revised heat losses in NCEP1 and NCEP2 (Fig. 2) are thus related to the wet bias in air humidity and a larger cold bias in SST relative to the cold bias in air temperature. In ECMWF, the larger cold bias of air temperature relative to the cold bias in SST along with the positive wind speed bias of 0.6 m s^{-1} is primarily responsible for its excessive sensible heat loss. The overestimated latent heat loss in ECMWF seems to be primarily related to high wind speed bias because the air–sea humidity gradient in ECMWF is close to the buoy value.

3) PIRATA

The COARE2.6a algorithm reduces the array-averaged latent heat loss by 25, 23, and 16 W m^{-2} for NCEP1, NCEP2, and ECMWF, respectively, thus largely reducing the original model heat flux biases. However, array-averaged overestimations of 16 and 8 W m^{-2} are still found in the revised ECMWF and NCEP2 latent heat losses. Also, the array-averaged revised NCEP1 sensible heat flux is still overestimated by 4 W m^{-2}. We did the similar analysis for all the buoys in the PIRATA array and found that the reductions in heat losses calculated using the COARE2.6a algorithm are persistent across the array, with the amounts of reduction in the subtropical buoys larger than those at the tropical buoys.

In PIRATA, the 10-m wind speeds in the three model analyses are underestimated systematically across the array, particularly on the equator, where the time mean bias reaches 1.5 m s^{-1} for NCEP1 and 1.1 m s^{-1} for NCEP2 and ECMWF. The low bias in model wind speed was also found in the tropical Pacific (Smull and McPhaden 1998), who noticed that the annual mean NCEP1 surface winds were weaker than those observed by the TOGA TAO moorings by about 1–2 m s^{-1} and the ECMWF Re-Analysis (ERA-15; with an atmospheric dynamical model similar to that in the operational ECMWF analysis-forecast system) displayed the similar bias but had 10%–20% smaller differences with the TAO values. Chelton (2001) also noticed a systematic low bias of 0.7 m s^{-1} in the tropical oceans in the ECMWF analysis compared to satellite measurements. The time mean SSTs from the model analyses match well with those from the buoys across the array except a warm bias of about 0.25°C shown in NCEP1 and NCEP2 at the northern equatorial buoys. The air temperature from ECMWF is close to the buoy value while it is biased low (by about 0.5°C) in NCEP1 in the northern and southern trade wind belts and biased slightly high on the equator in NCEP2. The cold bias in NCEP1 air temperature thus leads to a positive bias in air–sea temperature difference and to the overestimated bias in the revised sensible heat loss. Across the array the air humidity in ECMWF is persistently underestimated (by 1.0 g kg^{-1} for array average), which is also noticed in the tropical Pacific in ERA-15 (Klinker 1997). This dry bias is responsible primarily for the overestimated revised latent heat loss. NCEP2 displays broadly similar but smaller biases in air humidity, which lead to smaller biases in the revised latent heat flux. A slightly dry bias is also shown in NCEP1 across the array except in the northern and southern trade wind belts, where the NCEP1 air humidity is slightly overestimated.

In conclusion, significant biases in the time mean surface fields are shown in NCEP1, NCEP2, and ECMWF analyses as summarized in Table 1. The errors in bulk variables and the magnitudes of NWP heat flux biases related to inappropriate flux algorithms vary with regions and NWP models, which is synthesized in the last section of the article. NWP models are designed to forecast the day-to-day weather variations. In the following section, we evaluate the accuracy of the NWP model analyses in representing the observed variability characteristics.

4. Temporal variability comparison

The dominant timescale on which the variability of near-surface meteorological variables and air–sea heat fluxes occurs varies with geographic location and climate regime. During wintertime in the midlatitude western North Pacific and western North Atlantic, where strong cold air outbreaks are common, air–sea heat fluxes and atmospheric parameters show strong daily fluctuations; in regions that are influenced by subtropical high systems, such as in the eastern North and South Atlantic, the typical timescale of short-time atmospheric variability is about two weeks; in the Tropics, the coupled air–sea system exhibits primarily 2-week and longer-scale intraseasonal variability although diurnal cycle and high-frequency synoptic-scale variability play an important role in local ocean–atmosphere coupling and seasonal to interannual climate variability (Webster and Lukas 1992). In this section, we focus the temporal variability comparison on the dominant timescale exhibited in the deployments of experiments considered. Hence, we compare the daily variability in the coastal region experiments. In the Subduction Experiment and PIRATA, we use the 5-day running mean data (thus to eliminate the high-frequency variability) for temporal variability comparisons. Throughout this section, the multitaper method (MTM) of spectral analysis (Mann and Park 1993; Mann and Lees 1996) is employed to characterize the temporal variability of surface fields and the temporal coherence relationship between NWP analyses and buoy data. MTM is a technique designed to isolate signals in time series with a characteristic noise background, which is estimated by a ''robust'' procedure that is largely unbiased by the presence of signals embedded in the noise. All the spectral-related conclusions drawn in the following sections are based

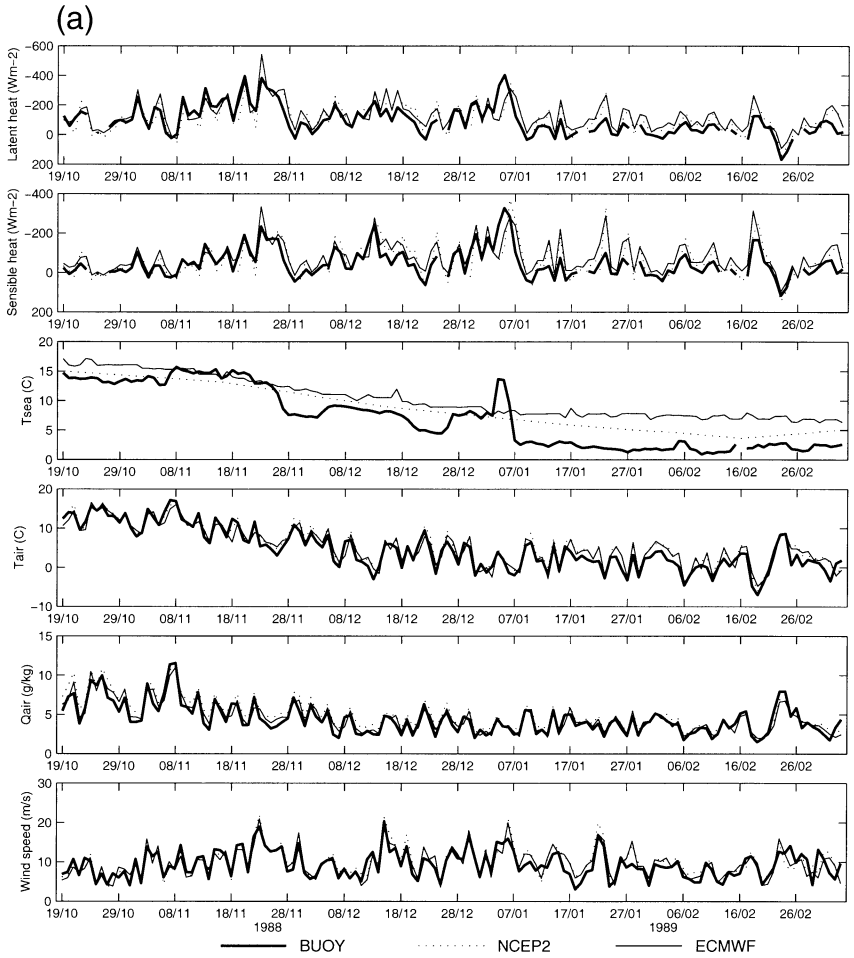

FIG. 4. (a) Daily series of latent heat flux, sensible heat flux, SST (T_{sea}), air temperature (T_{air}), air humidity (Q_{air}), and wind speed at (42.6°N, 61.2°W) for buoy data, NCEP2, and ECMWF. (b) Same as (a) except in ASREX 93 at (33.9°N, 69.8°W).

on the MTM analysis even though most of them are not shown with figures.

The temporal variability in surface fields is basically similar in NCEP1 and NCEP2, with the exception of SST. The NCEP2 SST variability is quite smooth while SST from NCEP1 exhibits short-time fluctuations, which are somewhat similar to those in operational ECMWF SST but lag the latter for several days in phase. The SST data in NCEP1 and NCEP2 reanalyses and operational ECMWF analysis all were produced from the same 7 days of in situ (ship and buoy) and satellite measurements using optimum interpolation (Reynolds and Smith 1994, hereafter RS94), but there are some differences between them. First, the sea ice boundary condition differs between the two. Secondly, for NCEP1 and ECMWF the daily SST was interpolated from the weekly RS94 product, but the interpolation/smoothing technique used in these two analyses is different, leading to the difference in their temporal fluctuation; for NCEP2 the interpolated daily RS94 SST was averaged to monthly and then filtered to eliminate bad points and reinterpolated to daily values, resulting in the smoothness in daily data. It is therefore expected that the NWP model analyses are not able to capture the day-to-day SST variation as we will see next. However, this section also reveals that the observed SST variability on timescales of 1–3 weeks is not correctly replicated. In this section, only NCEP2 is shown for the temporal variability comparison.

a. Daily mean comparison

Figure 4a shows the daily time series of heat fluxes and bulk variables during the SESMOOR deployment period. A few missing values in the heat flux series of Fig. 4a are due to nonconvergence of the iterative calculations in the flux algorithm. Our spectral analysis indicates that the 3–4-day timescale variability is dominant in buoy surface fields, particularly 10-m wind speed. In contrast, the buoy SST time series shows a gradual change in trend with a few cold and warm events embedded. The high-frequency variability in heat fluxes

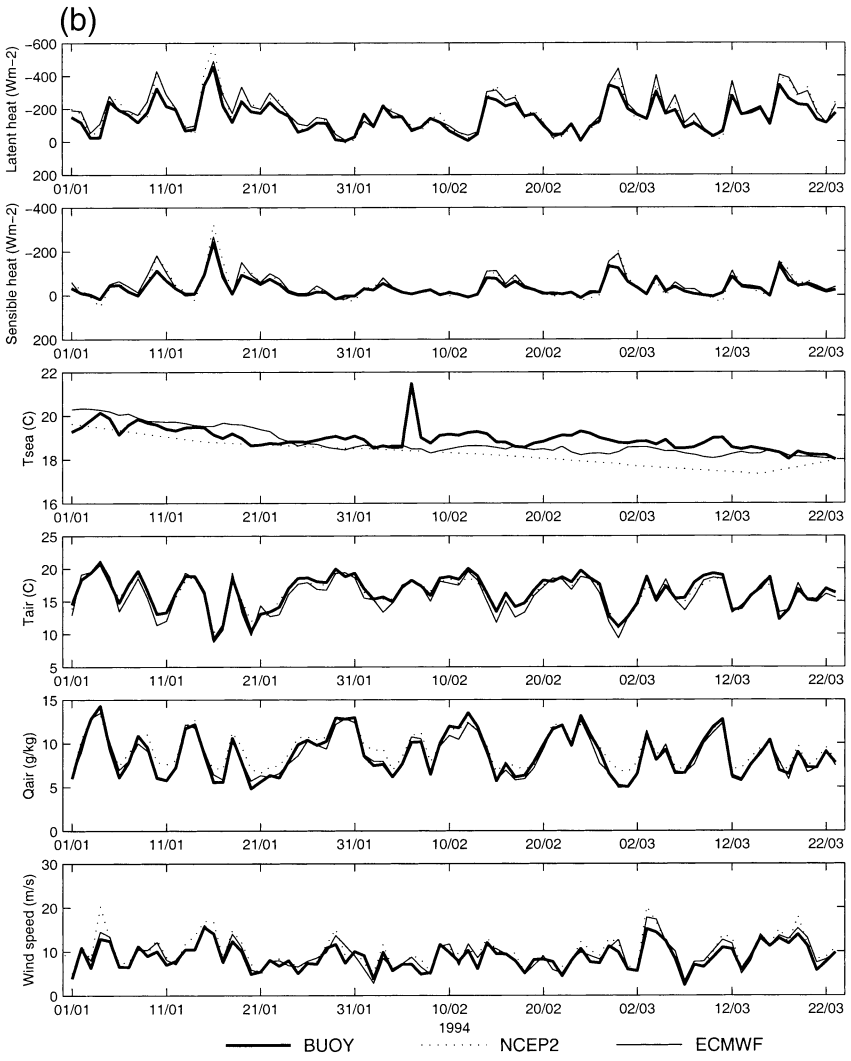

FIG. 4. (*Continued*)

is therefore determined by the strong variability of wind speed, air temperature, and humidity, but the warm/cold ocean state strongly affects the magnitude of heat fluxes. For example, with the decrease in SST from about 15°C in October–November of 1988 to about 2°C in February of 1989, the ocean latent (sensible) heat loss decreases from about 200 (100) to 30 (35) W m^{-2}. Except the failure of the NWP analyses to replicate the short-time SST fluctuations the observed high-frequency variability in near-surface meteorology and air–sea heat fluxes is significantly coherent with that in the model analyses. However, there are still some occasional mismatches of heat fluxes between the observation and the NWP analyses during the period we analyze. For example, the NWP heat flux variability is 1-day behind the buoy flux variability around 5 January 1989. This mismatch is caused by the inability of the NWP analyses to catch the warm SST spike on that day. However, we notice that despite the fact that the buoy SST drops by 10°C and the NCEP2 and ECMWF SSTs remain relatively constant around 5 January, the three show much the similar magnitude in the decrease of turbulent heat loss. This is because NCEP2 and ECMWF wind speeds fall by 6.3 and 6.7 m s^{-1}, respectively (in contrast to 3.0 m s^{-1} in buoy wind speed), which largely reduce the NWP turbulent heat losses. The very similar phenomena also occur around 5 February 1993 in ASREX93 (Fig. 4b).

In contrast to the 3–4-day timescale variability dominant in SESMOOR and CMO (not shown), the buoy data series in ASREX93 during the period January–March 1994 (Fig. 4b) all show 6–7-day timescale variability except the SST series, in which the dominant signal is the secular trend. Besides, the buoy 2-m humidity and 10-m wind speed also exhibit a signal of 2 weeks. It is noticed from Fig. 4b that the observed air temperature and humidity generally couple with SST on the timescale of 1–2 weeks although the amplitude of

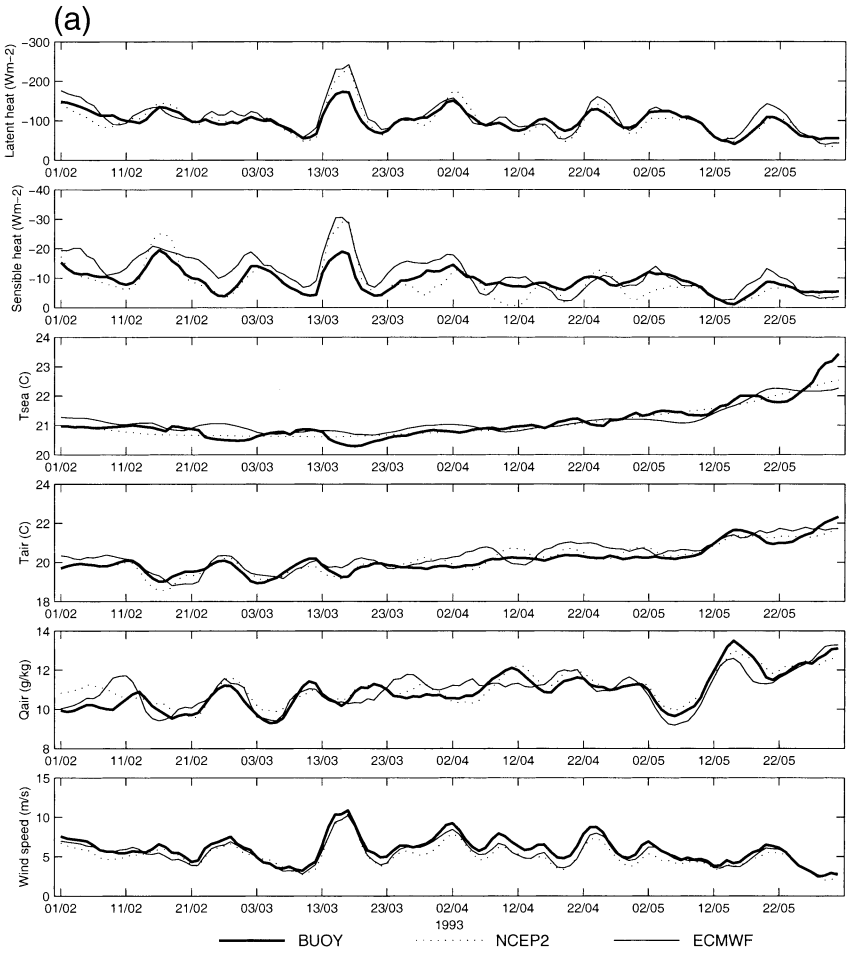

FIG. 5. (a) The 5-day running mean series of latent heat flux, sensible heat flux, SST (T_{sea}), air temperature (T_{air}), air humidity (Q_{air}), and wind speed in SESMOOR at buoy C (25.5°N, 29°W) of the Subduction Experiment for buoy data, NCEP2, and ECMWF. (b) Same as (a) except at (0°, 35°W) in the PIRATA array.

fluctuation in SST is much smaller than that in air temperature and humidity. For example, with the gradual increase in SST from 21 January to 31 January, air temperature became warmer and air specific humidity became higher. This phenomenon is not observed in SESMOOR or CMO, where SST varies slowly with time, and air temperature, humidity, and their high-frequency variability were determined mainly by the fast-moving westward cyclonic weather systems. However, similar to SESMOOR and CMO, in ASREX93 the NWP analyses successfully capture the short-time variability in heat fluxes and surface meteorology, except again in SST, whose synoptic-scale variability failed to be correctly reproduced. In other words, the NWP model analyses are able to replicate the variability in near-surface meteorology and thus the variability in heat fluxes despite the poor representation of SSTs prescribed in the NWP models as the external boundary forcing.

Compared to the coastal region experiments, the observed daily variability is not so well reproduced in the Subduction Experiment and the northern and southern trade winds of PIRATA (not shown), where the weather regime is relatively stable and supposed to be more easily simulated by the atmospheric dynamic models than that in the wintertime coastal regions. We thus speculate that the realistic capture of the strong variability in the NWP model analyses in the coastal region experiments is most probably because the NWP analysis-forecast systems assimilated a large quantity of in situ ship data and coastal land station data (Ebisuzaki et al. 1998).

We also compared the daily variability in the western equatorial Atlantic, where SST is warm and atmospheric convection is strong. It was found that the model analyses do not match the buoy variability on a large number of days although the PIRATA measurements were assimilated in the NWP analyses systems. Furthermore, the model analyses differ from each other considerably. Weller and Anderson (1996) indicated that the operational ECMWF analysis was not able to reproduce the

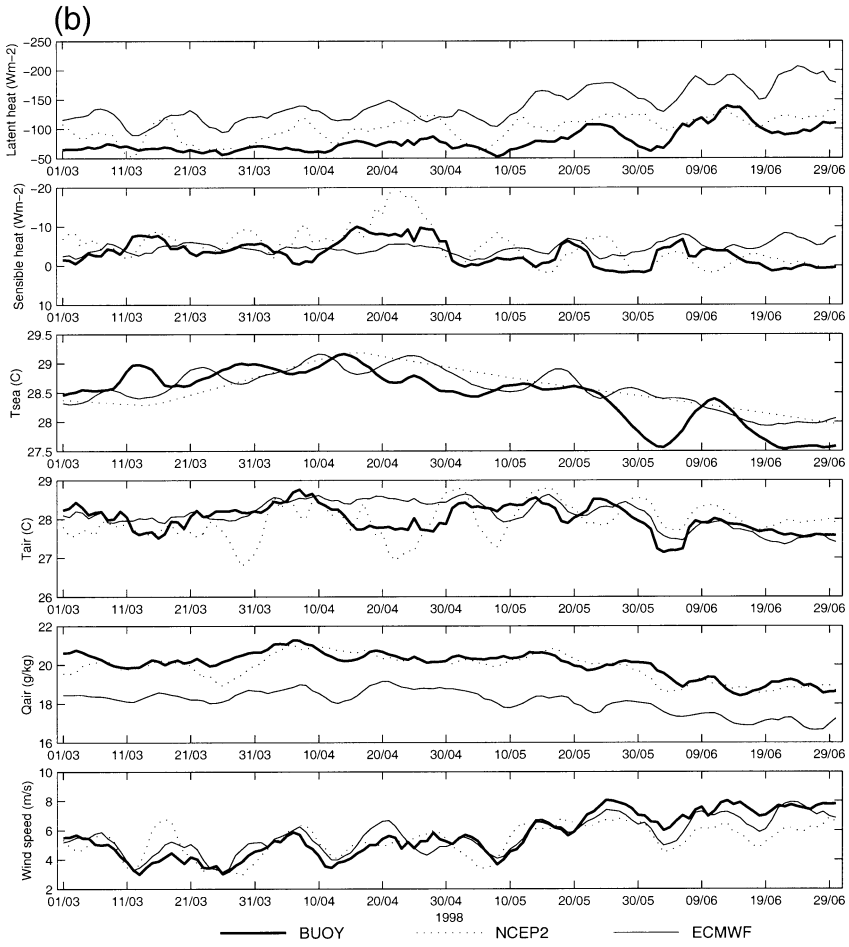

FIG. 5. (*Continued*)

deep convective events with the cycle of 2–3 days in the tropical Pacific. Here we do not include the conditions under which the NWP analyses fail to capture the high-frequency events in the tropical Atlantic, but we speculate that their inability may be partly related to the inappropriate parameterizations of clouds and other boundary layer processes in the NWP models as suggested by Wang and McPhaden (2001).

b. The 5-day mean comparison

The time series of 5-day running means for heat fluxes and meteorological variables in the period of February 1993–May 1993 at buoy C of the Subduction Experiment are shown in Fig. 5a. The variability in this season and at this location basically represents the average variability for the array. The observed variability occurs mainly on the timescale of 2 weeks with a relatively weak amplitude in SST. Throughout the whole time period both air temperature and humidity increased with SST, resulting in relatively stable latent and sensible fluxes. Our spectral analysis indicates that the temporal variability in air humidity and temperature between buoy data and NWP analyses is highly coherent, but the coherence is not so strong as that one between the buoy and the NWP 10-m wind speeds with regard to the width of the coherent spectrum as well as the confidence level. Visually we also see that the variability in NWP air humidity and air temperature is basically reproduced but not so well captured at periods with weak fluctuation (e.g., 15 March–10 May). For the heat fluxes, the model analyses are significantly coherent with the buoy data on the timescale of around 2 weeks, which in part could be due to the ability of the NWP analyses to reproduce the wind speed variability.

Most of the buoys in the tropical zone of PIRATA have a data length of less than 6 months. The buoy at position (0°N, 35°W) has 13-month continuous records. We therefore select that site as an example for the tropical weekly and longer timescale variability comparison. Figure 5b shows 5-day running mean time series for the buoy and model analyses at (0°N, 35°W) in the period of March–June 1998. This period corresponds to the transition of climate regime from the ITCZ to the southeast trade (Fig. 1), which leads to the decreases in SST, near-surface temperature, and humidity, and to the in-

crease in 10-m wind speed (Fig. 5a). As expected, the secular trends are dominant in the spectral curves of these variables. The spectral analysis on buoy measurements also exhibits a 2-week signal in humidity and wind and about 3-week signal in SST and latent heat flux. As shown in Madden and Julian (1994), the intraseasonal oscillation of 30–60 days that is pronounced in the western tropical Pacific and the eastern Indian Oceans is not so evident at this site in the tropical Atlantic. The pronounced short-time fluctuation exhibited in buoy SST at (0°N, 35°W) is not seen in the subtropical region (Figs. 5a,b) and wintertime coastal regions (Figs. 4a,b). Unfortunately, NCEP2 and ECMWF could not reproduce this variability at all, which may partly lead to the poor representation of air temperature and sensible heat flux variability (Fig. 5b) due to strong air–sea coupling in the Tropics. However, to some extent ECMWF is able to represent the dominant variability shown in buoy air humidity, wind speed, and latent heat flux at (0°N, 35°W), while in contrast NCEP2 is less able to reproduce these variables. Figure 6 shows such an example. Spectral analysis of the buoy 5-day running mean wind speed during March–June 1993 at (0°N, 35°W; Fig. 6a) reveals a secular trend (corresponding to the upward wind speed trend in Fig. 5b) and a 2-week signal, both of which are significant at 95% level. These two signals are found in the ECMWF spectrum (Fig. 6c) but with a larger amplitude in the 2-week signal and a smaller amplitude in the secular trend. NCEP2 shows the 2-week signal with only a marginal confidence level and the secular trend exhibited in buoy and ECMWF is not significant in NCEP2 analysis (Fig. 6b). Figure 6e also reveals that the spectral coherence between buoy and ECMWF wind data on the secular trend and timescale of 2 weeks is statistically significant with small phase lag. This suggests that the buoy wind variability on the dominant timescales is replicated in the ECMWF analysis. In contrast, the coherence of the NCEP2 wind with buoy wind is insignificant on these timescales (Fig. 6d), indicating the weak temporal relationship between them. We conducted the same analysis for NCEP1 and the result is somewhat similar to what we present for NCEP2.

5. Conclusions and discussion

Surface meteorological variables and turbulent heat fluxes in the NCEP1 and NCEP2 reanalyses and the operational ECMWF analysis are compared with high-quality moored buoy observations in regions of the Atlantic including the eastern North Atlantic, the coastal regions of the western North Atlantic, and the Tropics.

The time mean oceanic heat loss from the model analyses is systematically overestimated in all the regions. The overestimation in latent heat loss ranges from about 14 W m^{-2} (13%) in the eastern subtropical North Atlantic to about 29 W m^{-2} (30%) in the Tropics to about 30 W m^{-2} (49%) in the midlatitude coastal areas, where the overestimation in sensible heat flux reaches about 20 W m^{-2} (60%). Depending upon region and NWP model, these systematic overestimations are either reduced, or change to underestimations, or remain unchanged when the COARE flux algorithm is used to recalculate the fluxes. The bias in surface meteorological variables, one of the major factors related to the biases in the revised NWP heat fluxes, varies with region and NWP analysis. Generally the temperature and humidity biases in the coastal regions are much larger than other regions. In the extratropical regions, NCEP1 and NCEP2 generally show a wet bias, which is mainly responsible for the underestimation in the revised NWP latent heat loss. In the Tropics a dry bias is found in the NWP analyses, particularly in ECMWF and NCEP2, which contributes to the overestimation in the revised NWP latent heat loss. Compared to NCEP1, NCEP2 shows less cold bias in 2-m air temperature and thus less biased sensible heat flux; NCEP2 also shows less humid bias in 2-m humidity in the extratropical regions but more dry bias in 2-m humidity in the Tropics, either of which leads to more biased latent heat flux in NCEP2. All the NWP analyses display a low wind bias in the tropical Atlantic and the eastern subtropical North Atlantic but a positive bias in the wintertime coastal regions.

Despite the significant biases in the NWP surface fields and the poor representation of short-time SST variability, the NWP models are able to represent the dominant short-time variability in other basic variables and thus the variability in heat fluxes in the wintertime coastal regions of the western North Atlantic (on timescales of 3–4 days and 1 week) and the northern and southern subtropical regions (on a timescale of about 2 weeks), but ECMWF and particularly NCEP analyses do not represent well the 2–3-week variability in the tropical Atlantic.

Zeng et al. (1998) used tropical Pacific measurements to compare six different flux algorithms including the ones in NCEP1 and ECMWF. They found that the too large heat roughness lengths in these flux algorithms are primarily responsible for excessive turbulent heat losses. In this study, the COARE2.6a algorithm reduced the latent heat loss overestimation for ECMWF in the Subduction Experiment and PIRATA, for NCEP1 and NCEP2 in CMO and PIRATA. Hence, the use of the COARE2.6a algorithm with the NWP variables in those experiments brings the revised heat flux closer to buoy value. Flux algorithms with appropriate roughness lengths can indeed reduce the turbulent heat flux overestimation as seen in Renfrew et al. (2002) and Smith et al. (2001). However, this study also indicates that in the coastal region experiments the COARE2.6a algorithm did not change significantly the biases in ECMWF heat fluxes. Also, in the Subduction Experiment, SESMOOR, and ASREX93, the latent heat loss overestimation biases in NCEP1 and NCEP2 turn out to be underestimation biases when the COARE2.6a algorithm

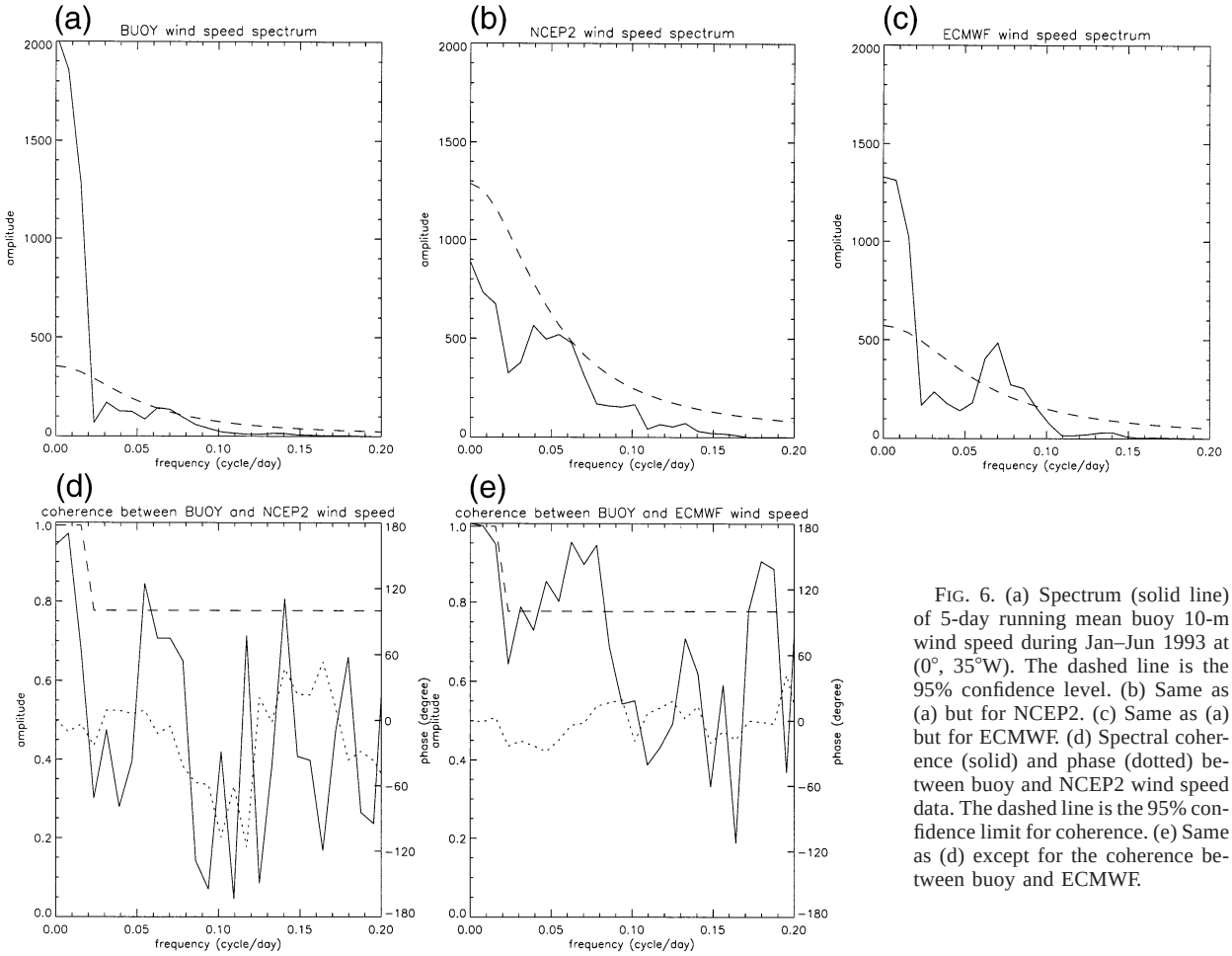

FIG. 6. (a) Spectrum (solid line) of 5-day running mean buoy 10-m wind speed during Jan–Jun 1993 at (0°, 35°W). The dashed line is the 95% confidence level. (b) Same as (a) but for NCEP2. (c) Same as (a) but for ECMWF. (d) Spectral coherence (solid) and phase (dotted) between buoy and NCEP2 wind speed data. The dashed line is the 95% confidence limit for coherence. (e) Same as (d) except for the coherence between buoy and ECMWF.

is used. For example, in the Subduction Experiment, the original NCEP1 latent heat loss showed the bias of +12 W m^{-2} while the revised NCEP1 one exhibited the bias of −16 W m^{-2}. We also used Zeng et al.'s (1998) flux algorithm to recalculate NWP fluxes and similar results are obtained. All these findings suggest that the quality of surface heat fluxes depends not only on the performance of the NWP flux algorithm but also on the quality of NWP surface meteorological variables.

The NCEP1, NCEP2, and ECMWF datasets we analyzed were produced from the atmospheric dynamical model-based data assimilation system. The quality of analyses from such systems relies largely on the dynamical model's performance. Even though the TAO buoy data in the equatorial Pacific were assimilated in the analysis system, the analyses still showed biases of low wind speed and cold air temperature (Wang and McPhaden 2001). The failure of the NWP analyses to capture short-time events and intraseasonal variability previously observed in the tropical Pacific (Weller and Anderson 1996) was seen in the tropical Atlantic by this study. All these results suggest that large uncertainties may exist in the NWP models in their representation of cloud and boundary layer processes. No doubt, the quality of basic meteorological variables from the NWP model analysis system also depends on the quantity and quality of assimilated historical data. The realistic description of high-frequency synoptic events in the wintertime coastal regions by the NWP analyses is probably because the NWP analysis-forecast systems assimilate more in situ data at and near the coast. However, as revealed in this study, the significant bias in SST analyses in the coastal regions of the western North Atlantic largely affects the magnitude in air–sea heat exchange. The misrepresentation of short-time SST variability in the NWP analyses indicated in this study can affect other meteorological variables and their variability through air–sea coupling particularly in the Tropics. Thus, there is a pressing need for real-time daily SST with fine spatial resolution (Thiebaux et al. 2001) for the NWP analysis-forecast system.

Acknowledgments. The Subduction Experiment mooring array and the coastal region experiment moorings were deployed by the Upper Ocean Processes Group, Woods Hole Oceanographic Institution (WHOI).

The authors acknowledge N. Galbraith and A. Plueddemann at WHOI, who did the buoy data preparation. The PIRATA array data were obtained via the Internet and were prepared by the TAO Office of the Pacific Marine Environmental Laboratory. The authors would also like to acknowledge the Data Support Section at NCAR for providing the ECMWF and NCEP data. The technical assistance of K. Huang, M. Caruso, and B. Gaffron at WHOI is acknowledged. The first author thanks Dr. M. Mann at the University of Virginia for providing the multitaper method of spectral analysis. The comments from two reviewers and Dr. T. Joyce at WHOI were critical to the quality of this paper. Acknowledgment is also made to NCAR, which is sponsored by the National Science Foundation, for supporting part of the computing time used in this research. This work is supported by the NOAA CLIVAR-Atlantic program under Grant NA06GP0453.

REFERENCES

Bolton, D., 1980: The computation of equivalent potential temperature. *Mon. Wea. Rev.,* **108,** 1046–1053.

Bradley, E. F., C. W. Fairall, J. E. Hare, and A. A. Grachev, 2000: An old and improved bulk algorithm for air–sea fluxes: COARE2.6A. Preprints, *14th Symp. on Boundary Layer and Turbulence,* Aspen, CO, Amer. Meteor. Soc., 294–296.

Chelton, D. B., 2001: Scatterometer-based assessment of surface wind field analyses from the Eurpoean Centre Medium-Range Weather Forecasts. *Proc. WCRP/SCOR Workshop on Intercomparison and Validation of Ocean–Atmosphere Flux Fields,* WCRP-115, WMO/TD-1083, Potomac, MD, WCRP, 135–141.

Crescenti, G. H., S. A. Tarbell, and R. A. Weller, 1991: A compilation of moored current meter data and wind recorder data from the severe environment surface mooring (SESMOOR). Woods Hole Oceanographic Institution Tech. Rep. WHOI-91-18, Woods Hole, MA, 59 pp.

Curry, J. A., C. A. Clayson, W. B. Rossow, R. Reeder, Y.-C. Zhang, P. J. Webster, G. Liu, and R.-S. Sheu, 1999: High-resolution satellite-derived dataset of the surface fluxes of heat, freshwater, and momentum for the TOGA COARE IOP. *Bull. Amer. Meteor. Soc.,* **80,** 2059–2080.

Donlon, C. J., T. J. Nightingale, T. Sheasby, J. Turner, I. S. Robinson, and W. J. Emery, 1999: Implications of the oceanic thermal skin temperature deviation at high wind speeds. *Geophys. Res. Lett.,* **26,** 2505–2508.

Ebisuzaki, W., M. Chelliah, and R. Kistler, 1998: NCEP/NCAR Reanalysis: Caveats. *Proc. First WCRP Int. Conf. on Reanalyses,* WCRP-104, WMO/TD-876, Silver Spring, MD, WMO, 81–84.

ECMWF, 1994: The description of the ECMWF/WCRP level III—A global atmospheric data archive. ECMWF Tech. Report, European Centre for Medium-Range Weather Forecasts, Reading, United Kingdom, 72 pp.

Fairall, C. W., E. F. Bradley, D. P. Rogers, J. B. Edson, and G. S. Young, 1996: Bulk parameterization of air–sea fluxes for Tropical Ocean Global Atmosphere Coupled Ocean–Atmosphere Response Experiment. *J. Geophys. Res.,* **101,** 3747–3764.

Galbraith, N. R., A. Gnanadesikan, W. M. Ostrom, E. A. Terray, B. S. Way, N. J. Williams, S. H. Hill, and E. Terrill, 1996: Meteorological and oceanographic data during the ASREX III field experiment: Cruise and data report. Woods Hole Oceanographic Institution Tech. Rep. 96-10, Woods Hole, MA, 247 pp.

——, A. Plueddemann, S. Lentz, S. Anderson, M. Baumgartner, and J. Edson, 1999: Coastal mixing and optics experiment moored array data report. Woods Hole Oceanographic Institution Tech. Rep. WHOI-99-15, Woods Hole, MA, 162 pp.

Halpern, D., M. H. Freilich, and R. A. Weller, 1999: ECMWF and *ERS*-1 surface winds over the Arabian Sea during July 1995. *J. Phys. Oceanogr.,* **29,** 1619–1623.

Jones, C. S., D. M. Legler, and J. J. O'Brien, 1995: Variability of surface fluxes over the Indian Ocean: 1960–1989. *Global Atmos.–Ocean Syst.,* **3,** 249–272.

Josey, S. A., 2001: A comparison of ECMWF and NCEP–NCAR surface heat fluxes with moored buoy measurements in the subduction region of the Northeast Atlantic. *J. Climate,* **14,** 1780–1789.

Kalnay, E., and Coauthors, 1996: The NCEP/NCAR 40-Year Reanalysis Project. *Bull. Amer. Meteor. Soc.,* **77,** 437–471.

Kanamitsu, M., W. Ebisuzaki, J. Woolen, J. Potter, and M. Fiorion, 2000: An overview of NCEP/DOE Reanalysis-2. *Proc. Second Int. Conf. on Reanalyses,* Reading, United Kingdom, WMO, 1–4.

Klinker, E., 1997: Diagnosis of the ECMWF model performance over the tropical oceans. Preprints, *Seminar on Atmosphere–Surface Interaction,* Reading, United Kingdom, ECMWF, 53–66.

Legler, D. M., I. M. Navon, and J. J. O'Brien, 1989: Objective analysis of pseudostress over the Indian Ocean using a direct-minimization approach. *Mon. Wea. Rev.,* **117,** 709–720.

Madden, R. A., and P. R. Julian, 1994: Observations of the 40–50-day tropical oscillation: A review. *Mon. Wea. Rev.,* **122,** 814–837.

Mann, M. E., and J. Park, 1993: Spatial correlations of interdecadal variation in global surface temperatures. *Geophys. Res. Lett.,* **20,** 1055–1058.

——, and J. M. Lees, 1996: Robust estimation of background noise and signal detection in climatic time series. *Climatic Change,* **33,** 409–445.

Moyer, K. A., and R. A. Weller, 1997: Observations of surface forcing from the Subduction Experiment: A comparison with global model products and climatological datasets. *J. Climate,* **10,** 2725–2742.

Renfrew, I. A., G. W. K. Moore, P. S. Guest, and K. Bumke, 2002: A comparison of surface layer and surface turbulent flux observations over the Labrador Sea with ECMWF analyses and NCEP reanalyses. *J. Phys. Oceanogr.,* **32,** 383–400.

Reynolds, R. W., and T. M. Smith, 1994: Improved global sea surface temperature analyses using optimum interpolation. *J. Climate,* **7,** 929–948.

Servain, J., A. J. Busalacchi, M. J. McPhaden, A. D. Moura, G. Reverdin, M. Vianna, and S. E. Zebiak, 1998: A Pilot Research Moored Array in the Tropical Atlantic (PIRATA). *Bull. Amer. Meteor. Soc.,* **79,** 2019–2031.

Smith, S. R., D. M. Legler, and K. V. Verzone, 2001: Quantifying uncertainties in NCEP reanalyses using high-quality research vessel observations. *J. Climate,* **14,** 4062–4072.

Smull, B. F., and M. J. McPhaden, 1998: Comparison of NCEP/NCAR and ECMWF reanalyzed fields with TOGA TAO buoy observations over the tropical Pacific. *Proc. First WCRP Int. Conf. on Reanalyses,* Geneva, Switzerland, World Meteorological Organization, 227–330.

Thiebaux, J., B. Katz, W. Wang, E. Roger, R. Kistler, and G. White, 2001: New sea-surface temperature analysis implemented at NCEP. *Proc. WCRP/SCOR Workshop on Intercomparison and Validation of Ocean–Atmosphere Flux Fields,* WCRP-115, WMO/TD-1083, Potomac, MD, WCRP, 90–94.

Wang, W., and M. J. McPhaden, 2001: What is the mean seasonal cycle of surface heat flux in the equatorial Pacific? *J. Geophys. Res.,* **106,** 837–857.

Webster, P. J., and R. Lukas, 1992: TOGA COARE: The Coupled Ocean–Atmosphere Response Experiment. *Bull. Amer. Meteor. Soc.,* **73,** 1377–1416.

Weller, R. A., and S. P. Anderson, 1996: Surface meteorology and air–sea fluxes in the western equatorial Pacific warm pool during the TOGA Coupled Ocean–Atmosphere Response Experiment. *J. Climate,* **9,** 1959–1990.

——, M. F. Baumgartner, S. A. Josey, A. S. Fischer, and J. Kindle,

1998: Atmospheric forcing in the Arabian Sea during 1994–1995: Observations and comparisons with climatology and models. *Deep-Sea Res. II,* **45,** 1961–1999.

Yu, L., B. Sun, and R. A. Weller, 2001: New daily air–sea flux fields for the Atlantic Ocean—Preliminary results. *Proc. WCRP/SCOR Workshop on Intercomparison and Validation of Ocean–Atmosphere Flux Fields*, WCRP-115, WMO/TD-1083, Potomac, MD, WCRP, 175–178.

Zeng, X., M. Zhao, and R. E. Dickinson, 1998: Intercomparison of bulk aerodynamic algorithms for the computation of sea surface fluxes using TOGA COARE and TAO data. *J. Climate*, **11,** 2628–2644.